A COMPARISON OF THE OPTIMAL MULTIPLIER IN POLAR AND RECTANGULAR COORDINATES

BY

JOSEPH EUZEBE TATE

B.S., Louisiana Tech University, 2003

THESIS

Submitted in partial fulfillment of the requirements
for the degree of Master of Science in Electrical Engineering
in the Graduate College of the
University of Illinois at Urbana-Champaign, 2005

Urbana, Illinois

ABSTRACT

Studies of the optimal multiplier (or optimal step size) modification to the standard Newton-Raphson load flow have mainly focused on highly stressed and unsolvable systems. This paper extends these previous studies by comparing performance of the Newton-Raphson load flow with and without optimal multipliers for a variety of unstressed, stressed, and unsolvable systems. Also, the impact of coordinate system choice in representing the voltage phasor at each bus is considered. In total, four solution methods are compared: the Newton-Raphson algorithm with and without optimal multipliers using polar and rectangular coordinates. This comparison is carried out by combining analysis of the optimal multiplier technique with empirical results for 2-bus, 118-bus, and 10 274-bus test cases. These results indicate that the polar Newton-Raphson load flow with optimal multipliers is the best method of solution for both solvable and unsolvable cases.

TABLE OF CONTENTS

1. INTRODUCTION

1.1 Motivation

While the Newton-Raphson (NR) load flow [1] has served the power industry well, one of the fundamental problems with the NR load flow has always been the possibility of divergence during solution. Divergence can occur when solving the load flow equations for a variety of reasons:

- Infeasibility, i.e., no solution to the load flow equations exists
- The system solution is too close to the boundary of unsolvability
- The initial guess of the solution is too far from the actual solution

Infeasibility has become more of a problem in the electricity grid since restructuring occurred. This is due to the increased utilization of existing transmission resources without any significant increase in transmission investment [2]. These activities have led to a system that is operated very close to the region of unsolvability, defined as the set of system parameters such that the power flow does not have a solution [3, 4]. The space of system parameters, divided into solvable and unsolvable regions, is illustrated in Figure 1.1. When contingency analysis is performed on systems that are already very close to the unsolvability boundary, it is not uncommon to find system configurations that are unsolvable.

The problem of having a solution that is too close to the boundary of infeasibility is due to the near-singularity of the Jacobian used in the NR load flow. This problem is particularly prevalent when performing maximum loadability studies. Several techniques have been developed for the sole purpose of avoiding difficulties at the boundary of infeasibility with the standard NR load flow, most notably the continuation load flow methods. However, even the continuation methods can have difficulties when the initial guess at a solution is too far from the actual solution. In particular, when the predicted point taken as a result of the predictor step is too far from the solution, the corrector step (load flow solution) may be too far from the solution point, leading to divergence [5].

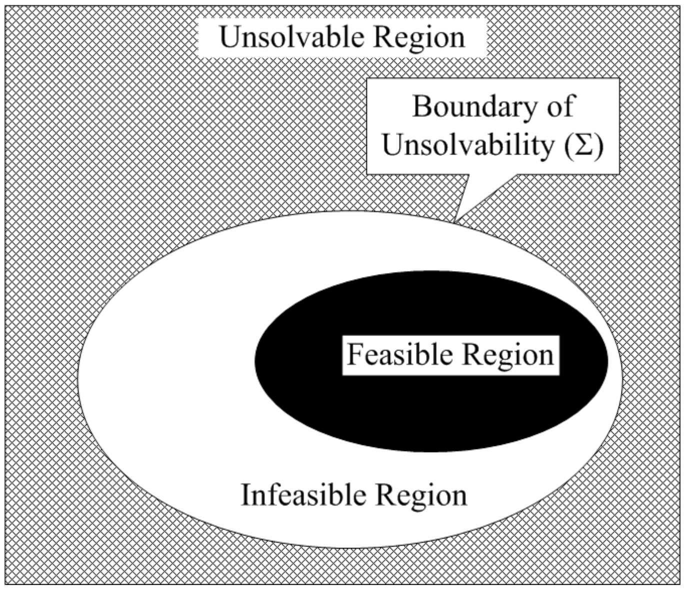

Figure 1.1 - Power flow security regions [3]

The problem of the initial guess has always plagued the NR method and is one of its primary disadvantages. While the NR method of solving nonlinear equations is well-established to exhibit quadratic convergence in a region that is sufficiently close to the final solution, the behavior of the NR load flow when the initial guess is far away from the solution is very unpredictable. In fact, it has been shown that the load flow problem has fractal regions of convergence [6].

1.2 Methods of Controlling Divergence

Divergence of the NR load flow has several drawbacks. First, if the solution process diverges, nothing has been gained. Accordingly, the faster the solution can be stopped, the more time is saved. Also, it is difficult to know whether the divergence of the NR load flow is due to poor initial conditions or unsolvability of the power system. Accordingly, many load flow solution methods have been developed to contain or eliminate divergence of the standard NR load flow.

Reference [7] provides an excellent summary of methods used to mitigate divergence in load flow solutions by step size optimization. These methods and others have been shown to prevent divergence of the load flow solution in many cases.

1.3 Desirable Characteristics of a Load Flow Solution Method

While nondivergence is an excellent characteristic to have in a load flow solution algorithm, any method used for load flow solutions must be both fast and robust for any type of system, whether the system is unstressed, stressed, or unsolvable. Unfortunately, little attention has been paid to the behavior of these nondivergent methods for normally convergent, unstressed systems in addition to stressed and unsolvable systems.

One candidate load flow solution method which has been shown to possess both speed and robustness for stressed and unsolvable systems is the optimal multiplier (OM) modification to the standard NR load flow. The OM load flow was first conceived in rectangular coordinates [8], but then extended using the same concepts to polar coordinates. Reference [9] provides full details on how the method of [8] has been extended to polar coordinates with varying degrees of success. Although the OM load flow has been extended to polar coordinates, comparison to the equivalent formulation in rectangular coordinates has not been performed.

1.4 Overview

The lack of comparison between the two coordinate systems is a crucial oversight, for the speed and robustness of a given load flow algorithm depend not only on the choice of algorithm but also on the choice of coordinate system used to represent the voltage phasors at the system buses [10]. Without such a comparison, load flow software developers must simply choose one coordinate system and hope that it is the best. While developers may end up getting lucky with their choice, it would be better to have evidence supporting the use of one system over the other.

Accordingly, the remainder of this thesis presents a direct comparison of four methods—the OM load flow and NR load flow using polar and rectangular coordinates. Chapter 2 provides the notation and formulation used in the standard NR load flow and the OM load flow solution methods. Chapter 3 discusses the relative advantage and disadvantages of using rectangular or polar coordinates to represent the voltage phasors at each bus. Chapter 4 provides case studies demonstrating the performance of the different solution methods on 2-bus, 118-bus, and 10 274-bus cases. Chapter 5 reviews the results from the case studies and provides analysis of the results. Finally, Chapter 6 provides the main conclusion of this work, namely that the polar formulation of the OM load flow provides the best combination of speed and robustness for unstressed, stressed, and unsolvable systems.

2. THE NR AND OM LOAD FLOW METHODS

2.1 The Coordinate Systems and the Load Flow Equations

In the polar NR load flow, the complex voltage phasor at each bus is represented using polar coordinates:

$$\hat{V}_i = \left|\hat{V}_i\right| \angle \theta_i \tag{2.1}$$

For the rectangular load flow formulation, the voltage phasor at each bus is represented using rectangular coordinates:

$$\hat{V}_i = e_i + j\, f_i \tag{2.2}$$

Figure 2.1 shows the relationships between the quantities in Equations (2.1) and (2.2):

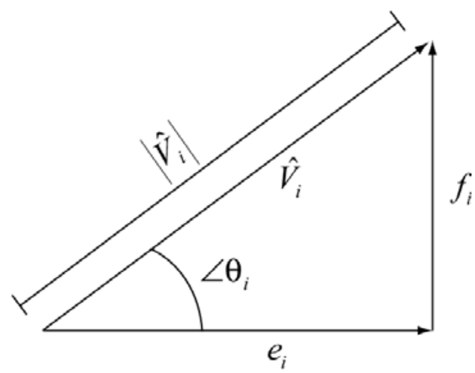

Figure 2.1 - Polar and rectangular representations of the bus voltage phasor

In the standard NR load flow, the set of load flow equations $\mathbf{f}(\mathbf{x}) = \mathbf{0}$ is solved. When polar coordinates are used for the voltage phasors, $\mathbf{f}(\mathbf{x})$ contains real and reactive power balance equations of the following forms:

$$\begin{aligned} P_i^{\text{Polar}}(\mathbf{x}) = \left|\hat{V}_i\right| \sum_{k \in \mathcal{C}_i} \left\{ \left|\hat{V}_k\right| \left(G_{ik} \cos(\theta_i - \theta_k) + B_{ik} \sin(\theta_i - \theta_k) \right) \right\} \\ + P_{load,i} - P_{gen,i} = 0 \end{aligned} \tag{2.3}$$

$$Q_i^{\text{Polar}}(\mathbf{x}) = \left|\hat{V}_i\right| \sum_{k \in \mathcal{C}_i} \left\{ \left|\hat{V}_k\right| \left(G_{ik} \sin(\theta_i - \theta_k) - B_{ik} \cos(\theta_i - \theta_k) \right) \right\} \\ + Q_{load,i} - Q_{gen,i} = 0 \tag{2.4}$$

where $\hat{Y}_{ij} = G_{ij} + jB_{ij}$, the complex admittance between buses i and j, and $\mathcal{C}_i$ denotes the set of all buses connected to bus i, including itself. The most important aspect of these equations as they relate to the OM load flow is the presence of transcendental functions in (2.3) and (2.4).

For the rectangular formulation, $\mathbf{f}(\mathbf{x})$ contains real power balance, reactive power balance, and voltage setpoint equations of the following forms:

$$P_i^{\text{Rect}}(\mathbf{x}) = \sum_{k \in \mathcal{C}_i} \left\{ e_i \left(G_{ik} e_k - B_{ik} f_k \right) + f_i \left(G_{ik} f_k + B_{ik} e_k \right) \right\} \\ + P_{load,i} - P_{gen,i} = 0 \tag{2.5}$$

$$Q_i^{\text{Rect}}(\mathbf{x}) = \sum_{k \in \mathcal{C}_i} \left\{ f_i \left(G_{ik} e_k - B_{ik} f_k \right) - e_i \left(G_{ik} f_k + B_{ik} e_k \right) \right\} \\ + Q_{load,i} - Q_{gen,i} = 0 \tag{2.6}$$

$$V_i^{\text{Rect}}(\mathbf{x}) = e_i^2 + f_i^2 - \left|\hat{V}_i\right|_{specified}^2 = 0 \tag{2.7}$$

It should be noted that the rectangular formulation uses an extra equation at each PV bus in the system (2.7) due to the need to maintain the specified voltage magnitude at these buses. As a result, the rectangular formulation has a larger equation and variable count than the polar formulation, with the difference equal to the number of voltage-controlled buses in the system. The salient characteristic of these equations with regard to the OM load flow is that all the state variables in (2.5)-(2.7) appear in quadratic terms. This leads to significant simplification of the Taylor series expansion of $\mathbf{f}(\mathbf{x})$ in rectangular coordinates.

2.2 The NR Load Flow

2.2.1 Formulation

The Newton-Raphson load flow [1] applies the well-known NR algorithm to the power flow equations (2.3)-(2.7). The NR method derivation begins with the first-order Taylor series expansion of $\mathbf{f}\left(\mathbf{x}\right)$ at an iteration ν:

$$\mathbf{f}\left(\mathbf{x}^{(\nu)}+\Delta\mathbf{x}^{(\nu)}\right)\approx\mathbf{f}\left(\mathbf{x}^{(\nu)}\right)+\mathbf{J}^{(\nu)}\Delta\mathbf{x}^{(\nu)} \tag{2.8}$$

where $\mathbf{J}^{(\nu)}$ is the Jacobian matrix of first-order partial derivatives of $\mathbf{f}\left(\mathbf{x}\right)$ with respect to $\mathbf{x}$:

$$\mathbf{J}^{(\nu)}=\left.\begin{bmatrix}\frac{\partial f_1}{\partial x_1} & \cdots & \frac{\partial f_1}{\partial x_n}\\ \vdots & \ddots & \vdots\\ \frac{\partial f_n}{\partial x_1} & \cdots & \frac{\partial f_n}{\partial x_n}\end{bmatrix}\right|_{\mathbf{x}=\mathbf{x}^{(\nu)}} \tag{2.9}$$

By setting the left-hand side of (2.8) equal to zero, $\Delta\mathbf{x}^{(\nu)}$ can be determined:

$$\Delta\mathbf{x}^{(\nu)}=-\left[\mathbf{J}^{(\nu)}\right]^{-1}\mathbf{f}\left(\mathbf{x}^{(\nu)}\right) \tag{2.10}$$

Once $\Delta\mathbf{x}^{(\nu)}$ has been determined, the states are updated and the iteration count is incremented by 1:

$$\begin{gathered}\mathbf{x}^{(\nu+1)}=\mathbf{x}^{(\nu)}+\Delta\mathbf{x}^{(\nu)}\\ \nu=\nu+1\end{gathered} \tag{2.11}$$

Given an initial condition $\mathbf{x}^{(0)}$ and setting $\nu=0$, (2.10) and (2.11) are evaluated repeatedly until a convergence criterion, e.g., $\left\|\mathbf{f}\left(\mathbf{x}^{(\nu)}\right)\right\|_{\infty}<\varepsilon$, is met.

2.2.2 Comments

The NR algorithm, in general, is very well behaved in regions very close to the solution, where the first-order Taylor series expansion is quite accurate. In regions close to the solution, the NR load flow exhibits quadratic convergence.

On the other hand, the algorithm can perform very poorly when the initial values $\mathbf{x}^{(0)}$ are far from a solution [11]. With poor starting conditions, the algorithm can diverge, leading to no solution even if the set of equations does have a solution. Such behavior can easily be observed by attempting to flat start an extremely large power system.

Also, it is possible that the set of equations $\mathbf{f}(\mathbf{x}) = \mathbf{0}$ are unsolvable, which also leads to divergence in the NR load flow. This undesirable behavior is particularly prevalent in contingency studies, where many changes to the system topology are carried out.

Finally, it is possible for an iteration to wind up where the Jacobian (2.9) is either singular or very close to singular. In these cases, inversion of the Jacobian (2.10) can lead to an inaccurate or incalculable $\Delta\mathbf{x}^{(\nu)}$. When this happens, the algorithm may diverge, giving meaningless results.

To combat the problems inherent in divergence of the NR algorithm, various modifications to (2.11) have been used in the past to control this behavior ([7] provides an excellent summary of several methods). One particularly promising method of controlling divergence is augmentation of the NR load flow with optimal multipliers.

2.3 The OM Load Flow

The optimal multiplier modification to the Newton-Raphson algorithm was first introduced for the rectangular formulation of the power flow equations [8]. Later, the same techniques were applied to the polar formulation [9]. Presented here is a general formulation of the optimal multiplier for any set of nonlinear equations $\mathbf{f}(\mathbf{x})$, from which the rectangular and polar formulations detailed in [8] and [12] can easily be obtained by setting $\mathbf{f}(\mathbf{x})$ to be the set of power flow equations (2.3)-(2.7). In the following chapter, specific comments on the rectangular and polar formulations as they relate to the OM load flow are presented.

2.3.1 Formulation

The basic idea behind the optimal multiplier technique is to choose the best scaling of the update vector $\Delta\mathbf{x}^{(\nu)}$ such that the norm of the second-order Taylor expansion of the mismatch equations is minimized. The technique is formulated by first modifying the standard NR update step (2.11):

$$\mathbf{x}^{(\nu+1)} = \mathbf{x}^{(\nu)} + \mu\Delta\mathbf{x}^{(\nu)} \tag{2.12}$$

where $\mu^{(\nu)}$ is a scalar value used to scale the update to $\mathbf{x}^{(\nu)}$ at an iteration ν and $\Delta\mathbf{x}^{(\nu)}$ is obtained using (2.10) as in the standard NR algorithm. Rewriting the Taylor series expansion for a single function $f_i(\mathbf{x})$ with the scalar multiplier $\mu^{(\nu)}$ and the second-order term of the Taylor expansion gives:

$$f_i\left(\mathbf{x}^{(\nu)}+\mu^{(\nu)}\Delta\mathbf{x}^{(\nu)}\right)\approx f_i\left(\mathbf{x}^{(\nu)}\right)+\mu^{(\nu)}\left(\sum_{k=1}^{n}\left.\frac{\partial f_i(\mathbf{x})}{\partial x_k}\right|_{\mathbf{x}=\mathbf{x}^{(\nu)}}\Delta x_k^{(\nu)}\right)$$
$$+\frac{\left(\mu^{(\nu)}\right)^2}{2}\left(\sum_{k=1}^{n}\sum_{m=1}^{n}\left.\frac{\partial^2 f_i(\mathbf{x})}{\partial x_m\partial x_k}\right|_{\mathbf{x}=\mathbf{x}^{(\nu)}}\Delta x_m^{(\nu)}\Delta x_k^{(\nu)}\right) \tag{2.13}$$

For convenience, several vectors are defined for the quantities on the right-hand side of (2.13):

$$\mathbf{a}^{(\nu)}=\begin{bmatrix} f_1\left(\mathbf{x}^{(\nu)}\right) \\ f_2\left(\mathbf{x}^{(\nu)}\right) \\ \vdots \\ f_n\left(\mathbf{x}^{(\nu)}\right)\end{bmatrix}=\mathbf{f}\left(\mathbf{x}^{(\nu)}\right) \tag{2.14}$$

$$\mathbf{b}^{(\nu)}=\begin{bmatrix} \sum_{k=1}^{n}\left.\frac{\partial f_1(\mathbf{x})}{\partial x_k}\right|_{\mathbf{x}=\mathbf{x}^{(\nu)}}\Delta x_k \\ \sum_{k=1}^{n}\left.\frac{\partial f_2(\mathbf{x})}{\partial x_k}\right|_{\mathbf{x}=\mathbf{x}^{(\nu)}}\Delta x_k \\ \vdots \\ \sum_{k=1}^{n}\left.\frac{\partial f_n(\mathbf{x})}{\partial x_k}\right|_{\mathbf{x}=\mathbf{x}^{(\nu)}}\Delta x_k \end{bmatrix}=\mathbf{J}^{(\nu)}\Delta\mathbf{x}^{(\nu)} \tag{2.15}$$

$$\mathbf{c}^{(\nu)}=\frac{1}{2}\begin{bmatrix} \sum_{k=1}^{n}\sum_{m=1}^{n}\left.\frac{\partial^2 f_1(\mathbf{x})}{\partial x_m\partial x_k}\right|_{\mathbf{x}=\mathbf{x}^{(\nu)}}\Delta x_m\Delta x_k \\ \sum_{k=1}^{n}\sum_{m=1}^{n}\left.\frac{\partial^2 f_2(\mathbf{x})}{\partial x_m\partial x_k}\right|_{\mathbf{x}=\mathbf{x}^{(\nu)}}\Delta x_m\Delta x_k \\ \vdots \\ \sum_{k=1}^{n}\sum_{m=1}^{n}\left.\frac{\partial^2 f_n(\mathbf{x})}{\partial x_m\partial x_k}\right|_{\mathbf{x}=\mathbf{x}^{(\nu)}}\Delta x_m\Delta x_k \end{bmatrix} \tag{2.16}$$

Equation (2.13), the quadratic approximation to $\mathbf{f}(\mathbf{x})$, can now be rewritten as

$$\mathbf{f}\left(\mathbf{x}^{(\nu)}+\Delta\mathbf{x}^{(\nu)}\right)\approx\mathbf{a}^{(\nu)}+\mu^{(\nu)}\mathbf{b}^{(\nu)}+\left(\mu^{(\nu)}\right)^2\mathbf{c}^{(\nu)} \tag{2.17}$$

Note that in general (2.17) does not hold with strict equality due to the third and higher order terms of the Taylor series expansion of $\mathbf{f}(\mathbf{x})$. However, in the rectangular formulation, because all terms in the Taylor series expansion of order three and above are zero, (2.17) holds with strict equality.

The optimal multiplier $\mu^{(\nu)}$ of the update vector $\Delta\mathbf{x}^{(\nu)}$ is determined by solving the following minimization problem:

$$
\begin{gathered}
\mathbf{F}(\mu) = \mathbf{a}^{(\nu)} + \mu^{(\nu)}\mathbf{b}^{(\nu)} + \left(\mu^{(\nu)}\right)^2 \mathbf{c}^{(\nu)} \\
\mu^{(\nu)} = \arg\min_{\mu\in[0,\infty]} \frac{1}{2}\left[\mathbf{F}(\mu)\right]^T \left[\mathbf{F}(\mu)\right] = \arg\min_{\mu\in[0,\infty]} \frac{1}{2}\left(\left\|\mathbf{F}(\mu)\right\|_2\right)^2
\end{gathered}
\tag{2.18}
$$

To determine the value of $\mu^{(\nu)}$ that solves the minimization problem in (2.18), the first order necessary condition of optimality is used:

$$
\left.\left(\frac{\partial}{\partial\mu}\frac{1}{2}\left(\left\|\mathbf{F}(\mu)\right\|_2\right)^2\right)\right|_{\mu^{(\nu)}} = 0 \tag{2.19}
$$

Equation (2.19) is a cubic equation in $\mu^{(\nu)}$:

$$
g_0 + g_1\mu^{(\nu)} + g_2\left(\mu^{(\nu)}\right)^2 + g_3\left(\mu^{(\nu)}\right)^3 = 0 \tag{2.20}
$$

where

$$
\begin{aligned}
g_0 &= \left[\mathbf{a}^{(\nu)}\right]^T \mathbf{b}^{(\nu)} \\
g_1 &= \left[\mathbf{b}^{(\nu)}\right]^T \mathbf{b}^{(\nu)} + 2\left[\mathbf{a}^{(\nu)}\right]^T \mathbf{c}^{(\nu)} \\
g_2 &= 3\left[\mathbf{b}^{(\nu)}\right]^T \mathbf{c}^{(\nu)} \\
g_3 &= 2\left[\mathbf{c}^{(\nu)}\right]^T \mathbf{c}^{(\nu)}
\end{aligned}
\tag{2.21}
$$

A closed form solution for (2.20) exists and is available in many mathematical handbooks, e.g. [13]. In the case of multiple roots, the smallest real root is chosen as the optimal multiplier [8].

2.3.2 Comments

As should be obvious from (2.12), the optimal multiplier is only able to scale $\Delta\mathbf{x}^{(\nu)}$; the direction of the update vector $\Delta\mathbf{x}^{(\nu)}$ is still based entirely on the first-order Taylor series expansion as in the standard NR algorithm. Accordingly, if the linearization of $\mathbf{f}(\mathbf{x})$ is poor, $\Delta\mathbf{x}^{(\nu)}$ may not indicate a very good direction. When the direction is not very good, the optimal multiplier provides little help in solving the system and can even slow down the solution.

For example, consider the single-variable equation

$$f(x) = x^4 + (x-1)^3 - 1 \tag{2.22}$$

This equation has only one real-valued solution: x = 1. To examine the behavior of the Newton-Raphson algorithm for this system, with and without the usage of optimal multipliers, a starting value of $x^{(0)} = 20$ is used. The function evaluation (2.22) at each iteration ν for both the standard NR and the NR with optimal multipliers is shown in Figure 2.2, plotted on a log scale. Note that the NR algorithm takes longer to converge to the solution when optimal multipliers are used. Also, the NR algorithm without optimal multipliers exhibits quadratic convergence starting with iteration 12, whereas the OM solution exhibits quadratic convergence starting with iteration 17—this is a sizable difference in convergence rate, as one of the main reasons to use the NR algorithm is the property of quadratic convergence.

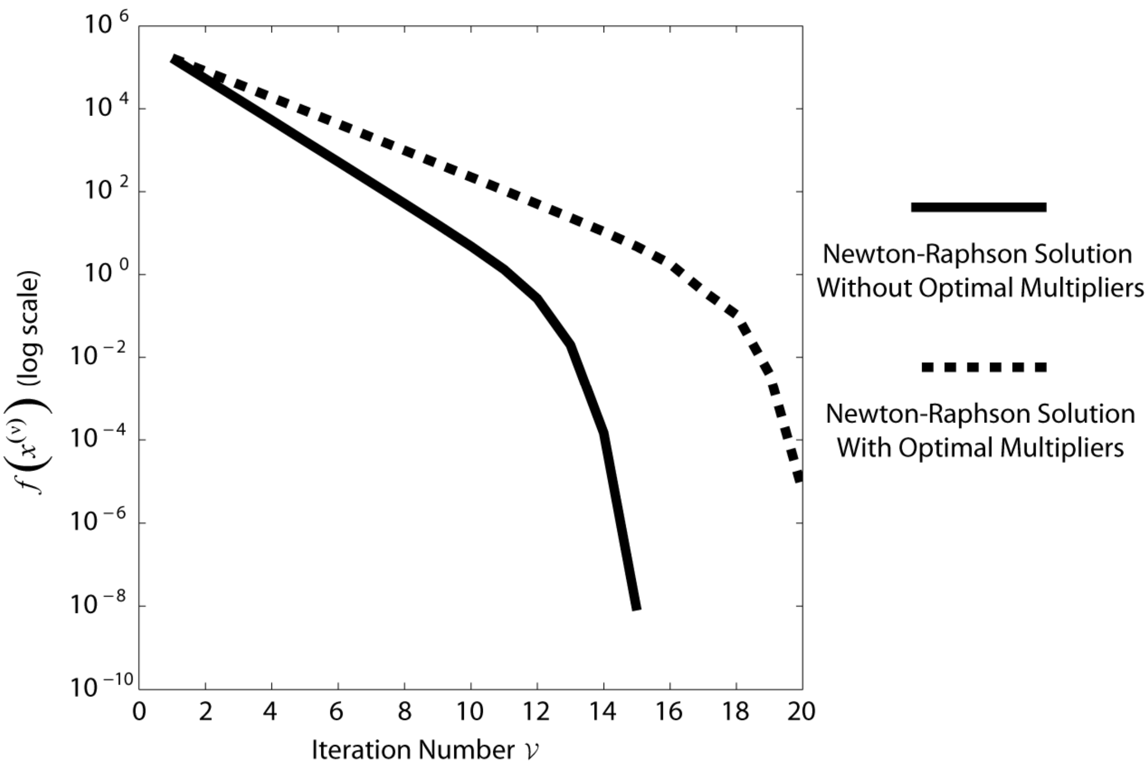

Figure 2.2 - Convergence of NR algorithm with and without optimal multipliers for solution of (2.22)

Figure 2.3 demonstrates why the optimal multiplier solution is slower—the values of $\mu^{(\nu)} < 1$ indicate that smaller steps are taken at each iteration in comparison to the standard NR algorithm. In fact, $\mu^{(\nu)}$ does not reach a steady value of 1 (thereby becoming equivalent to the standard NR algorithm) until iteration 17.

This behavior can be seen mathematically by examining the effect of large and small second-order terms on the optimal multiplier. The only information used when computing the optimal multiplier $\mu^{(\nu)}$ that is not used in computing the update vector $\Delta\mathbf{x}^{(\nu)}$ is the second-order term $\mathbf{c}^{(\nu)}$ (2.16). Because $\mathbf{c}^{(\nu)}$ is the second-order term of the Taylor expansion, $\mathbf{c}^{(\nu)}$ is zero if the load flow equations are exactly equal to their first-order Taylor series expansion, i.e., (2.8) holds with strict equality. When (2.8) is instead an approximation, $\mathbf{c}^{(\nu)}$ can take on a wide range of values.

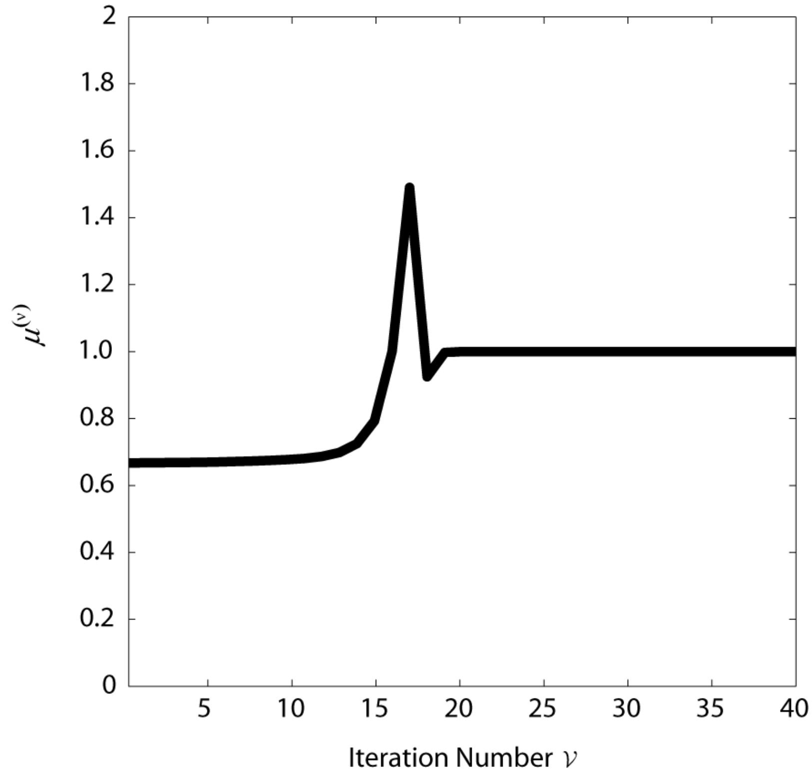

Figure 2.3 - Behavior of $\mu^{(\nu)}$ during solution of (2.22)

If $\mathbf{c}^{(\nu)}$ is zero, the optimal multiplier will be 1, just as if the NR algorithm were used. This can be seen by examining the minimization problem in (2.18) with $\mathbf{c}^{(\nu)}$ set equal to zero:

$$\begin{aligned}\mu^{(\nu)} &= \underset{\mu\in[0,\infty]}{\arg\min}\frac{1}{2}\left[\mathbf{a}^{(\nu)}+\mu^{(\nu)}\mathbf{b}^{(\nu)}\right]^T\left[\mathbf{a}^{(\nu)}+\mu^{(\nu)}\mathbf{b}^{(\nu)}\right] \\ &= \underset{\mu\in[0,\infty]}{\arg\min}\frac{1}{2}\left[\left(1+2\mu^{(\nu)}+\left(\mu^{(\nu)}\right)^2\right)\mathbf{a}^{(\nu)^T}\mathbf{a}^{(\nu)}\right] \\ &= \underset{\mu\in[0,\infty]}{\arg\min}\frac{1}{2}\left(\mu^{(\nu)}+1\right)^2\end{aligned} \tag{2.23}$$

This minimization problem has the trivial solution of $\mu^{(\nu)}=0$. On the other hand, if $\mathbf{c}^{(\nu)}$ is much larger in magnitude than $\mathbf{a}^{(\nu)}$ and $\mathbf{b}^{(\nu)}$, (2.18) can be reduced to

$$\mu^{(\nu)} \approx \underset{\mu\in[0,\infty]}{\arg\min}\frac{1}{2}\mu^2\left[\mathbf{c}^{(\nu)^T}\mathbf{c}^{(\nu)}\right] \tag{2.24}$$

The solution of (2.24) is $\mu^{(\nu)} \approx 0$, indicating that a large second-order term in the Taylor expansion leads to a very small optimal multiplier value.

A small optimal multiplier is desirable when attempting to solve unsolvable systems; it is precisely because $\mu^{(\nu)}$ takes on small values in such cases that divergence of the OM load flow is prevented. On the other hand, if small optimal multipliers occur when solving solvable systems, then the algorithm can take more iterations than the standard NR algorithm (which can be thought of as using a constant multiplier of 1). This behavior will be demonstrated in several case studies where the rectangular form of the OM load flow is used.

3. ADVANTAGES AND DISADVANTAGES OF EACH COORDINATE SYSTEM FOR THE OM LOAD FLOW

3.1 Advantages and Disadvantages of Polar Coordinates

The polar formulation has several advantages over the rectangular formulation when solving the load flow using the OM solution method. The polar form of the load flow equations exhibits excellent linearization characteristics, as demonstrated by both the Fast Decoupled Load Flow (FDLF) [14] and the usefulness of linear sensitivities in power system analysis such as power transfer distribution factors (PTDFs) [15]. Also, the polar formulation of the load flow equations has fewer equations to solve than the rectangular formulation. This can be significant for systems with relatively high percentages of voltage-controlled buses as in the IEEE 118-bus system.

However, there are also disadvantages to using the polar formulation instead of the rectangular formulation. The most significant drawback to the polar formulation is the presence of transcendental functions in the load flow equations. These functions lead to infinite order terms in the Taylor expansion, which makes (2.17) an approximation rather than a strict equality as in the rectangular formulation. As a result, the calculation of $\mu^{(\nu)}$ can be less accurate with the polar formulation than with the rectangular formulation. Also, the presence of sine and cosine functions in the polar load flow equations (2.3) and (2.4) leads to a more complex calculation of the second-order term $\mathbf{c}^{(\nu)}$ when compared to the calculation of $\mathbf{c}^{(\nu)}$ using rectangular coordinates. Fortunately, the calculation of $\mathbf{c}^{(\nu)}$ is still on the order of a mismatch calculation [9, 12].

Although there are some disadvantages to using the polar formulation, the case studies demonstrate that these disadvantages are outweighed by the advantages of using the polar formulation of the load flow equations and variables.

3.2 Advantages and Disadvantages of Rectangular Coordinates

In the original derivation of the OM solution method [8], several key advantages of the rectangular formulation are given. The greatest benefit of using the rectangular formulation results from the quadratic nature of the load flow equations when rectangular coordinates are used. Because all the state variables appear in quadratic terms in the equations, the third and higher order terms of the Taylor expansion are zero; this makes the Taylor series approximation used for optimal multiplier calculation (2.17) hold with strict equality. This can lead to greater accuracy in the calculation of $\mu^{(\nu)}$ relative to the polar formulation. Further, $\mathbf{c}^{(\nu)}$ is much easier to calculate than with the polar formulation, because in the rectangular formulation [8]

$$\mathbf{c}^{(\nu)} = \mathbf{f}\left(\Delta\mathbf{x}^{(\nu)}\right) \tag{3.1}$$

As a result, calculating the second-order term is just a matter of plugging $\Delta\mathbf{x}^{(\nu)}$ into the mismatch calculation routines instead of $\mathbf{x}^{(\nu)}$. Unfortunately, there are also several disadvantages to using the rectangular formulation. One problem with the rectangular formulation is the lack of widespread implementation of the NR load flow in rectangular coordinates [10], though at least one commercial load flow package does use the rectangular formulation by default [16]. The poor performance of the decoupled load flow in rectangular coordinates [17, 18] relative to the FDLF also indicates that the rectangular formulation may not have as good of a linearization as the polar formulation.

The extra voltage mismatch equation that must be satisfied at PV buses (2.7) can also lead to difficulties with the OM algorithm in rectangular coordinates [19]. The two-bus PV system examined in Chapter 4 clearly demonstrates how the extra equation can cause trouble with the OM algorithm.

4. CASE STUDIES

Because the convergence behavior of the NR load flow is difficult to analyze mathematically, particularly when the OM modification is used, empirical results are used to compare the two formulations.

A solution tolerance of 0.01 MW was used for each simulation. For unsolvable systems, the solution was stopped when the optimal multiplier dropped below 0.01, indicating that the solution had stalled at a constant mismatch. If any islanding occurred during outage studies, results were taken from the largest island.

In the following sections, ROM (POM) refers to solution using the OM load flow with rectangular (polar) coordinates, and RNR (PNR) refers to solution using the standard NR load flow without optimal multipliers with rectangular (polar) coordinates. In reporting the results for the case studies, several indices are used:

$$IC_{Rect}^{no\,opt}\left(IC_{Polar}^{no\,opt}\right) = \#\text{ of iterations to solve with RNR (PNR)} \tag{4.1}$$

$$IC_{Rect}^{opt}\left(IC_{Polar}^{opt}\right) = \#\text{ of iterations to solve with ROM (POM)} \tag{4.2}$$

$$\Gamma_{opt} = IC_{Rect}^{opt} - IC_{Polar}^{opt} \tag{4.3}$$

$$\Gamma_{no\,opt} = IC_{Rect}^{no\,opt} - IC_{Polar}^{no\,opt} \tag{4.4}$$

$$\Delta_{Rect} = IC_{Rect}^{no\,opt} - IC_{Rect}^{opt} \tag{4.5}$$

$$\Delta_{Polar} = IC_{Polar}^{no\,opt} - IC_{Polar}^{opt} \tag{4.6}$$

Values of Γ_{opt} ($\Gamma_{no\,opt}$) greater than zero indicate poorer performance of ROM (RNR) relative to POM (PNR). Values of Δ_{Rect} (Δ_{Polar}) greater than zero indicate poorer performance of ROM (POM) relative to RNR (PNR).

To examine the performance of the OM and NR solution methods under both coordinate systems, four systems are examined—a two bus system with a PV bus, a two bus system with a PQ bus, the IEEE 118-bus system, and a 10 274-bus system.

4.1 The Two-Bus PV System

4.1.1 System description

First, a two-bus system is examined to look at the effects of the voltage setpoint equation in rectangular coordinates. For this case, bus 2 has a voltage regulating generator in addition to a load, making bus 2 a voltage-regulated bus. The line connecting the two buses has constant parameters of R = 0.005 p.u. and X = 0.01 p.u. for all cases. A one-line diagram of this system is provided in Figure 4.1.

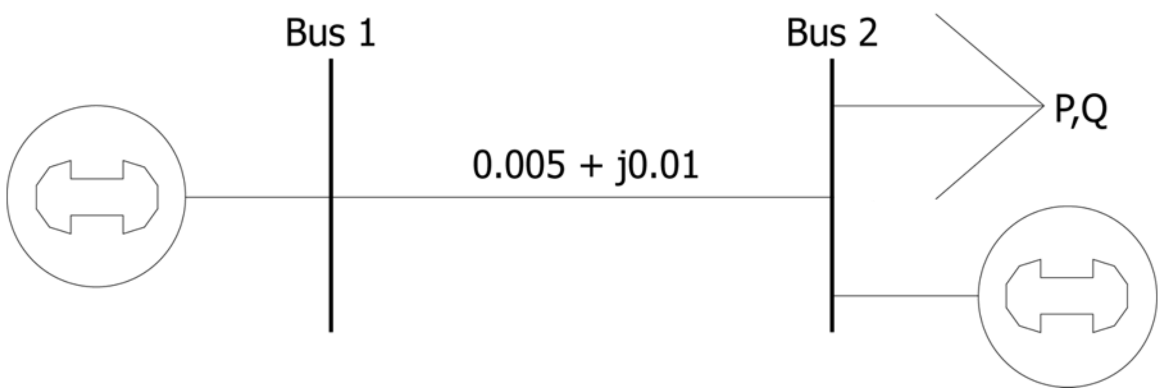

Figure 4.1 - Oneline diagram for the two-bus (PV) system

Because the voltage at bus 2 is regulated, there is only one equation ($P_2^{\text{Polar}}(\theta_2)$ = 0) and one unknown (θ_2) for this system in polar coordinates. The single equation in polar coordinates can be exactly solved analytically. Although the polar solution is trivial, this system clearly demonstrates some of the problems that can arise with ROM due to the voltage setpoint mismatch equation.

4.1.2 Case studies

In these cases the MW load at the second bus was varied from 0 to 4944 MW (maximum loadability) in increments of 1 MW, resulting in 4944 solvable cases. Due to the trivial solution of this system with polar coordinates, only the results for ROM and RNR are given in Table 4.1.

Table 4.1 - Number of iterations for two-bus (PV) solvable cases

	Min	Max	Avg
IC_{Rect}^{opt}	0	11	5.22
$IC_{Rect}^{no\ opt}$	0	9	3.71

	% of Cases		
	> 0	= 0	< 0
Δ_{Rect}	70.89%	27.57%	1.54%

Figure 4.2 shows the relationship between loading level and Δ_{Rect} for this system. The maximum value of Δ_{Rect} for the load range shown is 7, and the minimum value is -3.

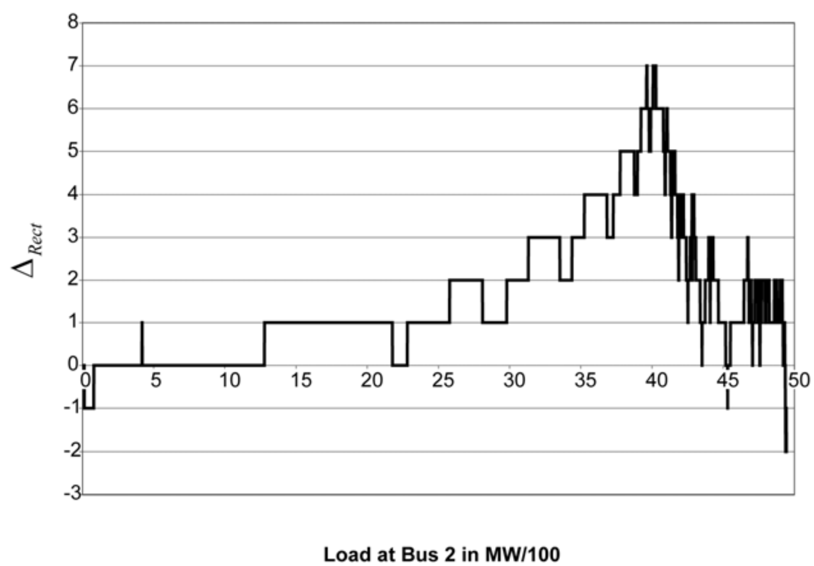

Figure 4.2 - Relationship between loading at bus 2 and Δ_{Rect} for the two-bus (PV) system

While Δ_{Rect} varied widely for these cases, ROM took more iterations in 71% of the cases. Although the ROM performed poorly for the vast majority of unstressed cases, as the system approached unsolvability the ROM did see some performance gains over RNR.

An unusual feature of Figure 4.2 is the large value of Δ_{Rect} for load levels around 4000 MW (about 80% of the maximum loading level of the system). A more detailed look at the system mismatch equations for this load level can help to explain why. Figures 4.3 and 4.4 are plots of the absolute value of the voltage setpoint mismatch equation (2.7) and the real power mismatch equation (2.5) at bus 2 as a function of the real and imaginary components of the bus 2 voltage over the ranges $0.75 \le e_2 \le 1.00$ and $-0.95 \le f_2 \le -0.4$. The goal of the power flow solution methods is to determine the point

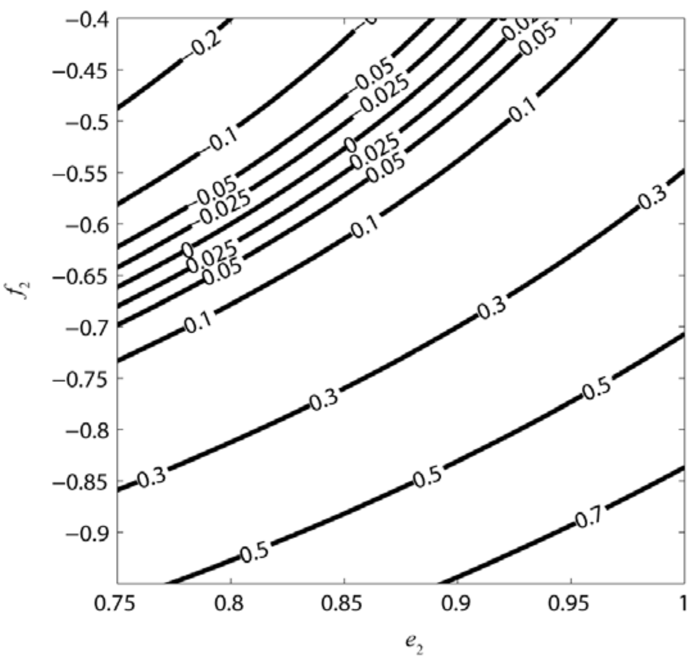

Figure 4.3 - Voltage mismatch (2.7) for the two-bus (PV) system with 4000-MW load

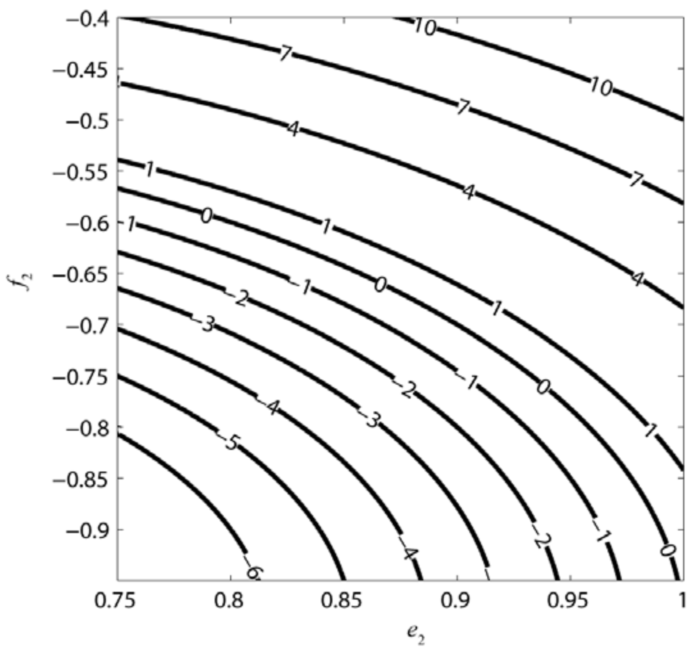

Figure 4.4 - Real power mismatch (2.5) for the two-bus (PV) system with 4000-MW load

where both mismatch equations are equal to zero. For a load of 4000 MW this occurs at V_2 = 0.8-0.6j. Clearly, evaluation of (2.5) results in values several orders of magnitude higher than (2.7) in the region of interest. As a result, the real power mismatch dominates both the shape and magnitude of the 2-norm of the total mismatch of the system, shown in Figure 4.5.

Also plotted in Figure 4.5 are the solution paths taken with RNR (solid line) and ROM (dashed line). Both iterations begin at a flat start of $e_2 = 1.0$, $f_2 = 0.0$ and end with $e_2 = 0.8$, $f_2 = -0.6$. Solving with the ROM clearly takes a longer path than solving with RNR.

The ROM solution method first sets the real power mismatch to zero, then attempts to correct the voltage mismatch while keeping the real power mismatch very close to zero. The cause of this behavior is precisely the magnitude difference mentioned above. Because the real power mismatch overpowers the voltage mismatch in the 2-

norm, the ROM solution method forces the solution to always stay very close to the region where the real power mismatch is zero. In this case, because the first iteration puts the voltage values at bus 2 far from the correct values for the voltage setpoint equation, the solution must wind along the $\left|P_2^{\text{Rect}}(\mathbf{x})\right|$ = 0 curve to get to the final solution. The tight, slow traversal of the $\left|P_2^{\text{Rect}}(\mathbf{x})\right|$ = 0 curve to arrive at the final solution is responsible for the difference in iteration counts between ROR and RNR.

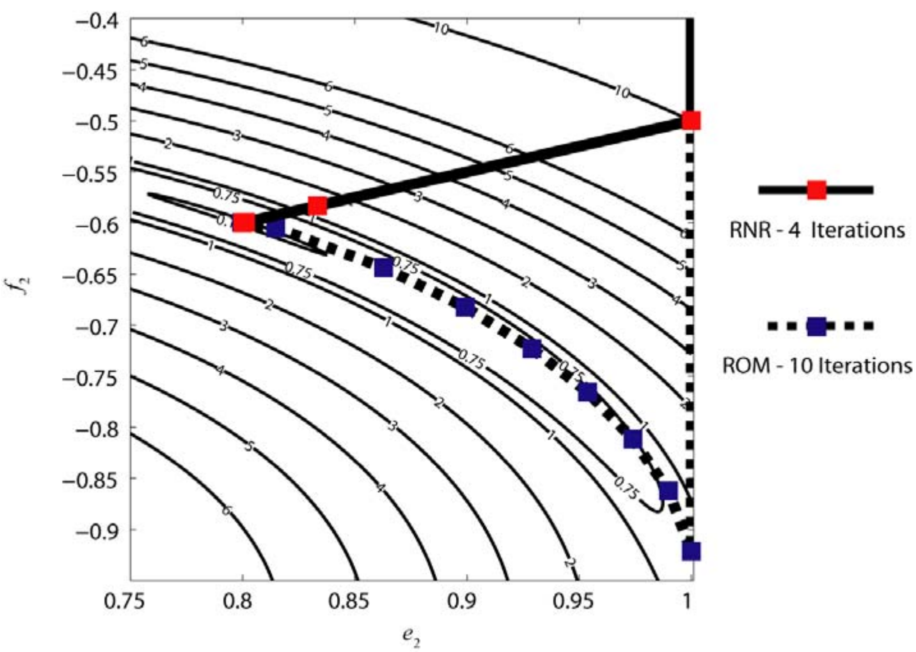

Figure 4.5 - Two-norm of the total mismatch for the two-bus (PV) system with 4000-MW load

In summary, the voltage mismatch equation does not present much of a challenge for the traditional NR load flow (RNR); convergence proceeds normally. On the other hand, the Newton-Raphson load flow with optimal multipliers (ROM) can encounter significant problems due to the vast differences of scale caused by the voltage setpoint equation at PV buses.

Heuristic methods of alleviating this problem, e.g., scaling the voltage equation by a fixed magnitude and disallowing small optimal multipliers, are discussed in [16] and [19]. Unfortunately, both of these methods have their own pitfalls. Scaling the voltage equation is problematic due to the difficulty in determining exactly how much to scale each voltage setpoint equation in large systems, and the rejection of small optimal multipliers can have the undesired side effect of causing more iterations to be performed for unsolvable systems.

4.2 The Two-Bus PQ System

4.2.1 System description

First, a simple two-bus system is examined in detail to demonstrate the behavior of the four solution methods. The system has a slack bus (bus 1) and an unregulated (PQ) load bus (bus 2) connected by a line with X held constant at 0.01 p.u. In all cases, initial conditions were taken to be the flat start values. A one-line diagram for this system is provided in Figure 4.6.

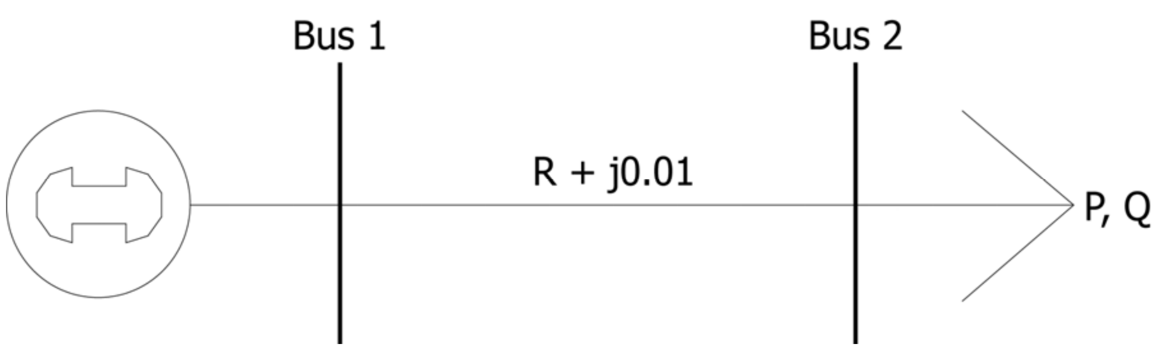

Figure 4.6 - One-line diagram for the two bus (PQ) system

4.2.2 Case studies

Cases were generated for this system by simultaneously varying three parameters: MW load from 0 to 2500 MW, MVar load from 0 to 2500 MVar, and R/X ratio from 0 to

2. Each range of system parameters (MW, MVar, and R) was broken up into 30 points, giving 27 000 total cases. Of the 27 000 total cases, 13 209 were solvable and the remaining 13 791 cases were not solvable. Comparison of the number of iterations needed to solve with the various methods is presented in Tables 4.2 and 4.3.

Table 4.2 - Number of iterations for two-bus (PQ) solvable cases

	Min	Max	Avg
IC_{Polar}^{opt}	1	6	2.56
IC_{Rect}^{opt}	1	7	3.25
$IC_{Polar}^{no\ opt}$	1	9	3.87
$IC_{Rect}^{no\ opt}$	1	9	3.90

	% of Cases		
	> 0	= 0	< 0
Γ_{opt}	66.76%	32.48%	0.76%
$\Gamma_{no\ opt}$	3.29%	96.28%	0.44%
Δ_{Rect}	0.00%	41.38%	58.62%
Δ_{Polar}	0.00%	11.57%	88.43%

Table 4.3 - Number of iterations for two-bus (PQ) unsolvable cases

	Min	Max	Avg
IC_{Polar}^{opt}	2	6	2.47
IC_{Rect}^{opt}	2	9	3.00

	% of Cases		
	> 0	= 0	< 0
Γ_{opt}	45.34%	54.14%	0.51%

POM provides significant gains over PNR, ROM, and RNR for these cases. Compared to PNR, POM takes an average of 51% fewer iterations for solvable cases, indicating significant performance gains when using the OM algorithm instead of the NR algorithm for these cases. RNR and ROM also performed worse than POM, taking an average of 52% and 27% more iterations, respectively.

4.2.3 ROM sensitivity to MVar loading and R/X ratio

Some sensitivity studies were also performed to gauge the effect of MVar loading and R/X line ratio on the performance of ROM relative to POM. To determine the effects of MVar loading, the R/X ratio of the line was held constant at 0.1 and the MW load at bus 2 was held constant at 1000 MW. Under these conditions, the MVar load at bus 2 was then varied from 0 MVar to 2300 MVar. The effect of the MVar load increase on Γ_{opt} can be seen in Figure 4.7. As can be seen in the figure, the amount of MVar load at bus 2 and Γ_{opt} are clearly related, with a correlation coefficient of 0.8815. This effect is most likely due to the strong correlation (0.836) between the MVar load at bus 2 and the angle shift on the system. As will be seen in the remaining cases, large angle shifts tend to negatively impact the ROM; this is indicated by higher values of Γ_{opt}.

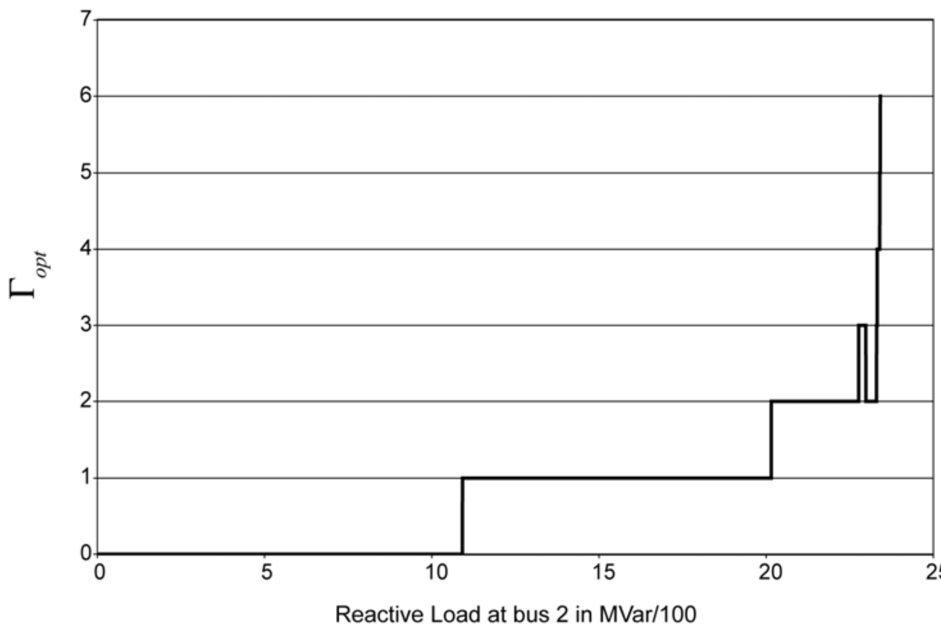

Figure 4.7 - The effect of MVar load on Γ_{opt} for the two-bus (PQ) case

An analysis of the effects of R/X ratio on Γ_{opt} was also conducted by holding the MW load at 1000 MW and the MVar load at 1000 MW. The R/X ratio was then varied from 0 to 1.472, corresponding to a variation of R from 0 to 0.01472 p.u. A strong dependence exists between the R/X ratio of the line connecting buses 1 and 2 and the rectangular iteration count minus the polar iteration count using optimal multipliers. This dependency is illustrated in Figure 4.8. As in the MVar loading cases, angle shifts are the most likely cause for the increase in Γ_{opt}; the correlation coefficient relating R to the angle shift is 0.994 for these cases.

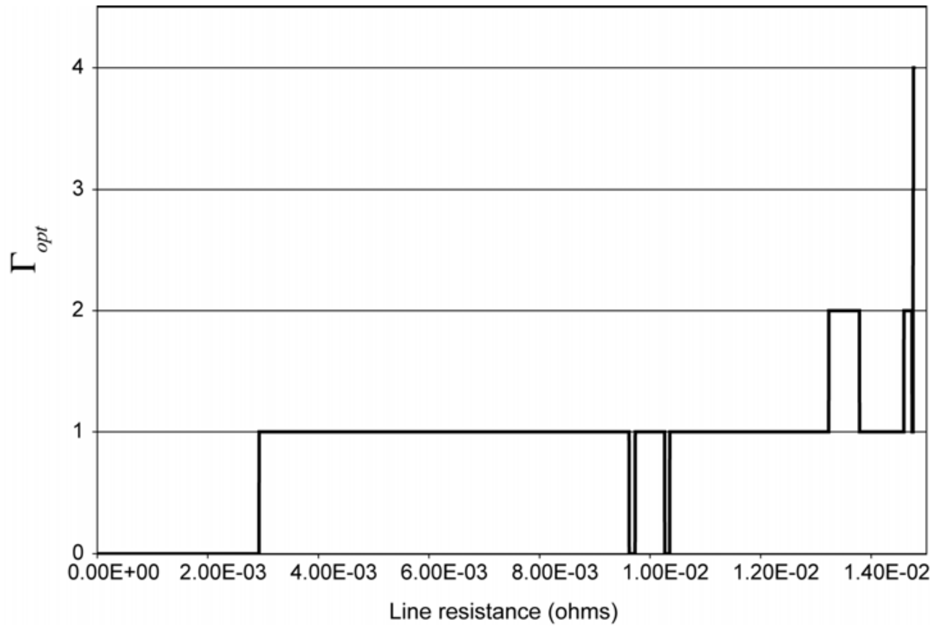

Figure 4.8 - The effect of R/X ratio on Γ_{opt} for the two-bus (PQ) case

4.3 The IEEE 118-Bus System

4.3.1 System description

The IEEE 118-bus system [20] is examined next. In order to compare the performance of the rectangular and polar formulations with this system, three difference studies were performed—all single outages, all double outages, and system-wide load scaling. Flat start values of $1\angle 0°$ p.u. were used as initial conditions for each case.

4.3.2 Case studies

4.3.2.1 Single and double outage studies

For the single outage study, all 186 lines in the system were outaged and the solution results were compared. The system was solvable for all single outages. For the double outage study, all 186 lines in the system were outaged in pairs for a total of 17 205 cases. One double outage case was unsolvable; in that case, the rectangular formulation took 5 iterations to stall and the polar formulation took 4. A comparison of the number of iterations required is given in Table 4.4 for all 17 390 solvable outage cases.

Table 4.4 - Number of iterations for 118-bus single and double outage cases

	Min	Max	Avg
IC_{Polar}^{opt}	3	4	3.001
IC_{Rect}^{opt}	3	6	3.166
$IC_{Polar}^{no\ opt}$	3	4	3.022
$IC_{Rect}^{no\ opt}$	3	6	4.012

	% of Cases		
	> 0	= 0	< 0
Γ_{opt}	16.44%	83.56%	0.00%
$\Gamma_{no\ opt}$	98.86%	1.14%	0.00%
Δ_{Rect}	0.05%	15.34%	84.61%
Δ_{Polar}	0.00%	97.81%	2.19%

Though the polar formulation did not see much improvement with the usage of optimal multipliers for the outage cases, IC_{Polar}^{opt} still has the lowest average of the four solution methods. The most notable aspect of these results, however, is that in 98.86% of the outage cases studied, PNR performed better than RNR. This is most likely due to high number of PV buses in this case—47 out of the 118 buses.

4.3.2.2 Load scaling

For the load scaling study, all real and reactive loads and generator outputs in the system were scaled uniformly by a multiplier. This multiplier ranged from 0.001 to 4.000 and was incremented by 0.001 for each case, giving a total of 4000 cases. The system was solvable for scaling between 0.001 and 3.187 and was unsolvable for scaling between 3.188 and 4.000. A comparison of the number of iterations required for these cases is summarized in Tables 4.5 and 4.6.

Table 4.5 - Number of iterations for solvable 118-bus load scaling cases

	Min	Max	Avg
IC^{opt}_{Polar}	1	7	2.82
IC^{opt}_{Rect}	1	7	3.24
$IC^{no\ opt}_{Polar}$	3	9	3.88
$IC^{no\ opt}_{Rect}$	3	9	3.94

	% of Cases		
	> 0	= 0	< 0
Γ_{opt}	63.85%	36.15%	0.00%
$\Gamma_{no\ opt}$	57.92%	42.08%	0.00%
Δ_{Rect}	26.26%	66.74%	7.00%
Δ_{Polar}	0.00%	85.00%	15.00%

Table 4.6 - Number of iterations for unsolvable 118-bus load scaling cases

	Min	Max	Avg
IC^{opt}_{Polar}	4	7	4.58
IC^{opt}_{Rect}	10	14	12.45

	% of Cases		
	> 0	= 0	< 0
Γ_{opt}	100%	0%	0%

Several aspects of the results for the load scaling are quite interesting. Most importantly, the average iteration count for POM is well below the other three methods, mirroring the results seen for the two bus PQ cases. Also, in all of the 813 unsolvable cases, POM stalled in fewer iterations than ROM. Because one of the primary purposes of using optimal multipliers is to quickly stall at a constant mismatch for unsolvable cases, the performance of the rectangular formulation for these unsolvable cases is of great concern.

ROM also performed worse relative to POM as the load multiplier was increased. In Figure 4.9, the solid line represents solvable cases and the dashed line represents unsolvable cases. Due to the large power transfers needed to satisfy the scaled load demand, large angle changes are occurring along with the load scaling; the norm of all angle changes on the system has a correlation coefficient of 0.91 with the load scaling. This suggests that large angle shifts are tied to the poor performance of ROM.

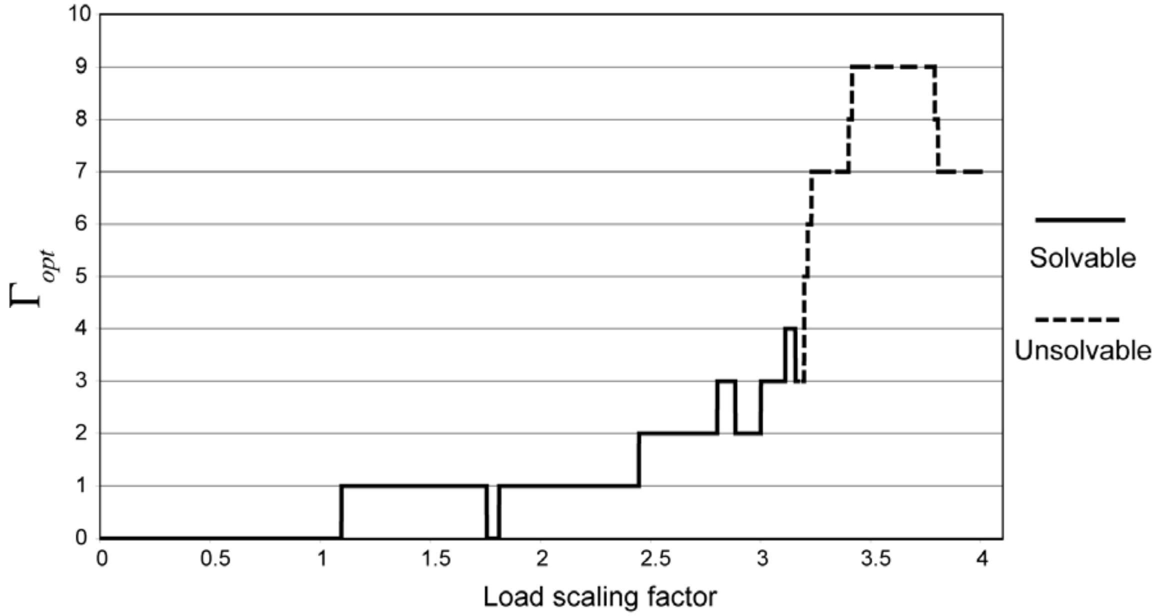

Figure 4.9 - Relation between the load scaling for the 118-bus system and Γ_{opt}

4.4 The 10 274-Bus System

4.4.1 Case studies

The final system examined is a 10 274-bus case. To test this case, the 500 lines carrying the most power were outaged and the solutions were examined. Of the 500 outage cases studied, 479 were solvable and 21 unsolvable. Comparison of the number of iterations for the solvable and unsolvable cases is provided in Tables 4.7 and 4.8, respectively.

Table 4.7 - Number of iterations for the solvable 10 274-bus outage cases

	Min	Max	Avg
IC^{opt}_{Polar}	2	5	2.61
IC^{opt}_{Rect}	3	85	6.06
$IC^{no\ opt}_{Polar}$	2	6	2.82
$IC^{no\ opt}_{Rect}$	3	7	3.38

	% of Cases		
	> 0	= 0	< 0
Γ_{opt}	70.15%	29.85%	0.00%
$\Gamma_{no\ opt}$	50.94%	48.85%	0.21%
Δ_{Rect}	16.28%	81.21%	2.51%
Δ_{Polar}	0.00%	79.12%	20.88%

Table 4.8 - Number of iterations for the unsolvable 10 274-bus outage cases

	Min	Max	Avg
IC_{Polar}^{opt}	3	8	5.10
IC_{Rect}^{opt}	11	144	68.33

	% of Cases		
	> 0	= 0	< 0
Γ_{opt}	100%	0%	0%

These results are simply terrible for the rectangular formulation. In 33 of the 479 solvable outage cases the rectangular formulation took at least 20 iterations to solve with the optimal multiplier. This accounts for the very large average value of IC_{Rect}^{opt} in Table 4.7. For the 21 unsolvable cases, Γ_{opt} was greater than zero in all cases. The rectangular formulation performed extraordinarily poorly for the unsolvable 10 274-bus cases. For instance, in three of the unsolvable cases, it took over 100 iterations for the rectangular optimal multiplier to drop below 0.01. Also, IC_{Polar}^{opt} has the lowest average iteration count of the four methods used to solve the load flow.

As in the 118 bus load scaling cases, there are some clear dependencies between angle shifts and problems with ROM in this system. Figure 4.10 provides a visual indicator of this dependence. Each dot in this figure represents a single solvable outage case. The correlation coefficient between the norm of the angle shifts and the differences in iteration counts is 0.98, based on the 479 solvable outages.

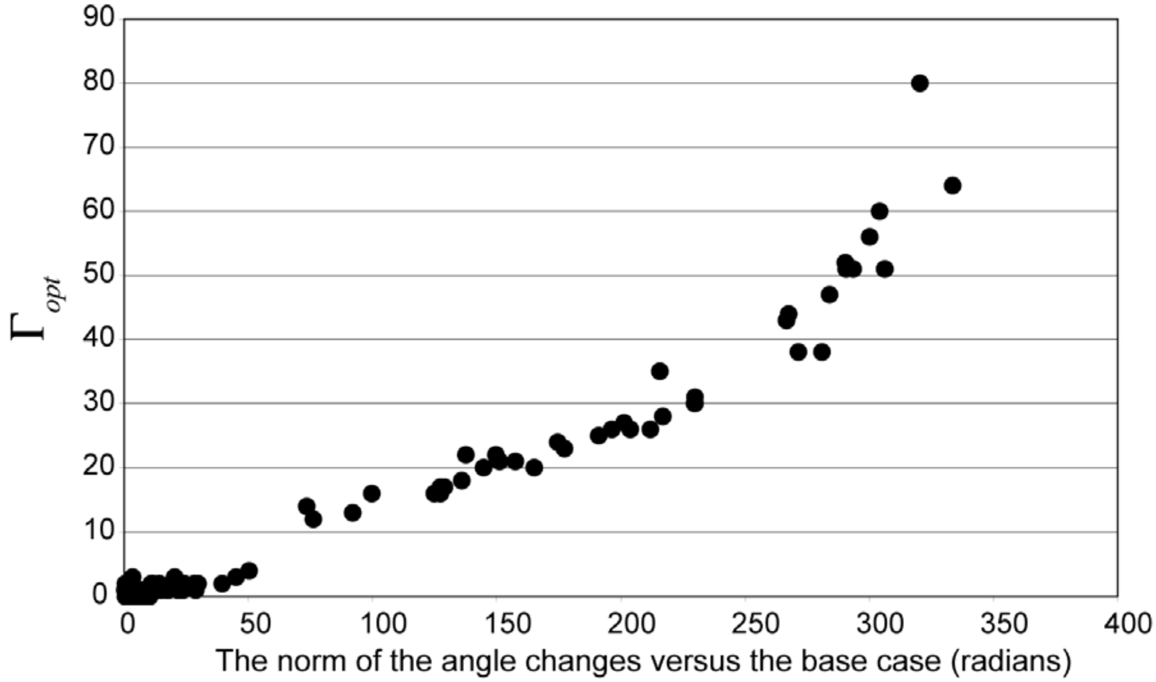

Figure 4.10 - Relationship between angle shifts and Γ_{opt} for the 10 274-bus system

5. CONCLUSIONS

5.1 Comments on Case Studies

5.1.1 The effects of angle shifts

For the systems examined in this paper, the greatest single indicator of poor performance with the rectangular formulation is the norm of the angle shifts for the system. The most likely cause of this dependence is that a change in angle is a curve in the rectangular solution space rather than a straight line. Also, as shown for the two-bus case in Figure 4.5, the rectangular formulation can have great difficulty in moving along a curve when the optimal multiplier is employed. For the polar formulation, on the other hand, changing angles is a linear movement with respect to the solution variables. This could help to explain why the polar formulation does not exhibit the same performance degradation when large angle shifts occur.

5.1.2 Average iteration count differences

For all three system sizes, the average value of IC_{Polar}^{opt} is less than the average value of IC_{Rect}^{opt}, indicating that the polar formulation usually performs better than the rectangular formulation when optimal multipliers are used. Also, in each set of cases, the average value of $IC_{Polar}^{no\ opt}$ is less than the average value of $IC_{Rect}^{no\ opt}$. This shows that the polar formulation routinely performs better than the rectangular formulation whether or not optimal multipliers are used. Finally, the average value of $IC_{Polar}^{no\ opt}$ is greater than the average value of IC_{Polar}^{opt} for all three system sizes, indicating that the polar usually receives some benefit from the usage of the optimal multiplier for solvable cases. On the other hand, the rectangular formulation does worse when optimal multipliers are used for several of the 10 274-bus cases and for the majority of the two-bus PV cases.

5.2 Choosing the Best Load Flow Algorithm

The case studies indicate that any advantages of using the rectangular formulation are offset by greater difficulties. These problems are particularly apparent as the system becomes highly stressed and unsolvable. At its best (the two bus PQ system) ROM took an average of 0.5 iterations more than POM in stalling for unsolvable cases. In the worst case, the 10 274-bus case, ROM took an average of 63 iterations more than POM to stall, including quite a few cases which took unreasonably long times (over 100 iterations) to stall.

On the other hand, the polar form of the OM algorithm performed very well throughout all simulations. The POM had a lower average iteration count than ROM for all systems, indicating that the polar coordinate system is the best choice if the OM algorithm is to be used. Also, POM behaved well for unsolvable systems by stalling quickly and not diverging. This behavior gives a clear advantage over both RNR and PNR when dealing with unsolvable systems, as the standard NR algorithm does not handle unsolvable systems gracefully. POM also had a lower average iteration count than PNR for every set of cases (and never had a higher iteration count than PNR for any single case). For these reasons, implementation of the optimal multiplier modification to the Newton-Raphson load flow with polar coordinates is recommended to get the fastest, most robust performance, regardless of system solvability or size.

REFERENCES

[1] W. F. Tinney and C. E. Hart, "Power flow solution by Newton's method," *IEEE Transactions on Power Apparatus and Systems*, vol. PAS-86, pp. 1449-1460, 1967.

[2] U.S.-Canada Power System Outage Task Force, "Final Report on the August 14, 2003 Blackout in the United States and Canada," 2003.

[3] T. J. Overbye, "Power flow measure for unsolvable cases," *IEEE Transactions on Power Systems*, vol. 9, pp. 1359-1365, 1994.

[4] S. Granville, J. C. O. Mello, and A. C. G. Melo, "Application of interior point methods to power flow unsolvability," *IEEE Transactions on Power Systems*, vol. 11, pp. 1096-1103, 1996.

[5] H.-D. Chiang, A. J. Flueck, K. S. Shah, and N. Balu, "CPFLOW: A practical tool for tracing power system steady-state stationary behavior due to load and generation variations," *IEEE Transactions on Power Systems*, vol. 10, pp. 623-634, 1995.

[6] J. S. Thorp and S. A. Naqavi, "Load-flow fractals draw clues to erratic behavior," *IEEE Computer Applications in Power*, vol. 10, pp. 59-62, 1997.

[7] M. D. Schaffer and D. J. Tylavsky, "A nondiverging polar-form Newton-based power flow," *IEEE Transactions on Industry Applications*, vol. 24, pp. 870-877, 1988.

[8] S. Iwamoto and Y. Tamura, "A load flow method for ill-conditioned power systems," *IEEE Transactions on Power Apparatus and Systems*, vol. PAS-93, pp. 1736-1743, 1981.

[9] L. M. C. Braz, C. A. Castro, and C. A. F. Murati, "A critical evaluation of step size optimization based load flow methods," *IEEE Transactions on Power Systems*, vol. 15, pp. 202-207, 2000.

[10] B. Stott, "Review of load-flow calculation methods," *Proceedings of the IEEE*, vol. 62, pp. 916-929, 1974.

[11] B. Stott, "Effective starting process for Newton-Raphson load flows," *Proceedings of the IEE*, vol. 118, pp. 983-987, 1971.

[12] L. M. C. Braz and C. A. Castro, "A new approach to the polar Newton power flow using step size optimization," presented at 29th North American Power Symposium, Laramie, WY, 1997.

[13] G. Korn and T. Korn, *Mathematical Handbook for Scientists and Engineers*. New York: McGraw Hill, 1968.

[14] B. Stott and O. Alsac, "Fast decoupled load flow," *IEEE Transactions on Power Apparatus and Systems*, vol. PAS-93, pp. 859-869, 1974.

[15] A. J. Wood and B. F. Wollenberg, *Power Generation, Operation, and Control*, 2nd ed. New York: Wiley-Interscience, 1996.

[16] R. P. Klump and T. J. Overbye, "Techniques for improving power flow convergence," presented at 2000 Power Engineering Society Summer Meeting, Seattle, WA, 2000.

[17] V. H. Quintana and N. Muller, "Studies of load flow methods in polar and rectangular coordinates," *Electric Power Systems Research*, vol. 20, pp. 225-235, 1991.

[18] L. Srivastava, S. C. Srivastava, and L. P. Singh, "Fast decoupled load flow methods in rectangular coordinates," *International Journal of Electrical Power & Energy Systems*, vol. 13, pp. 160-166, 1991.

[19] J. E. Tate and T. J. Overbye, "Rectangular power flow convergence using optimal multipliers," presented at 36th North American Power Symposium, Moscow, ID, 2004.

[20] "The Power System Test Case Archive," University of Washington, 2005, http://www.ee.washington.edu/research/pstca/.